ROZPRAWY INŻYNIERSKIE, ENGINEERING TRANSACTIONS. 31, 4, 501—524, 1983
Polska Akademia Nauk • Instytut Podstawowych Problemów Techniki

COMPLETE SOLUTIONS OF NONHOMOGENEOUS PLASTIC PLATES RESTING ON NONRIGID BEAMS

D. RYTWIŃSKA and M. KWIECIŃSKI (WARSZAWA)

A semi-inverse method is developed to obtain exact solutions to thin, rigid-ideally plastic plates resting on beams that are capable of deflecting together with the edges of the plates. The structural members of the plate-beam systems are assumed to obey the Huber–Mises yield condition. The structure is subjected to a transverse, uniformly distributed load and is point supported at the corners. New complete solutions are arrived at for isotropic plates in the shape of a square, a rectangle, a rhombus and a paallelogram. Orthotropic plates are also dealt with in the orthogonal situations. The obtained results make it possible to prescribe such a type of nonhomogeneity that the whole structure becomes plastic at the same intensity of load.

1. Introduction

In the case of such structures as thin plates with complex shapes and beam-plate structures, i.e. plates resting on a system of edge beams, the usual procedure is to assess the load-carrying capacity via either the lower bound approach or, more frequently, the upper bound approach. It is, at the same time, usually assumed that the beams remain rigid until the plastic motion begins, i.e. the edges of plates are not capable of deflecting during the loading process [7, 8, 9, 16, 21].

The purpose of this paper is to develop a semi-inverse method leading to exact solutions for rigid-perfectly plastic thin plates resting on nonrigid beams. Isotropic and orthotropic nonhomogeneous plates dealt with are made of the Huber–Mises material. Transverse, uniformly distributed load is applied. The structures are point-supported at the corners. Nonhomogeneity can result either from variable thickness of the plate or from its internal structure such as fibrous reinforcement. Civil engineering applications will be mainly that of reinforced concrete slab-beam systems.

All the basic assumptions concerning limit analysis of ideally plastic plates will be here accepted. Those are: the thicknesses of both plates and beams are small enough to apply the Love–Kirchhoff kinematical hypothesis, the strains remain small and the deflections prior to collapse are such that the equilibrium equations can be referred to the underformed configurations, the yield condition is taken as a plastic potential so the associated flow law is employed and only those stresses enter the yield criterion that generate the bending and the twisting moments.

To obtain a complete solution, an ultimate load must be found associated with both the kinematically admissible mechanism of incipient plastic motion and the statically admissible distribution of generalized stresses throughout the structure considered. A suitable system of the first-order partial differential equations has to be solved. Its type clearly depends on the type of the yield condition assumed. In the case of a yield condition linear with respect to the bending and the twisting moments all three types of equations can be present — elliptic, parabolic and hyperbolic. For instance, the Tresca yield condition was dealt with in [6, 15, 2]. When the rectangular, Johansen yield condition is employed, the elliptic equations are excluded. Such plates have received much attention in the literature [1, 3, 11, 12, 13, 14, 17, 18].

However, both the Tresca and the Huber–Mises yield conditions superimpose rather stringent constraints on the curvature rates and the class of surfaces of deflection rates is mainly limited to the developable ones. Such surfaces can satisfy neither the statical nor the kinematical boundary conditions accompanying the the sagging edges of plates. Thus the nonlinear, Huber–Mises yield condition, leading to the ellipticity of equations [8], will be used throughout, enabling exact solutions to be arrived at for the considered structural systems. A suitable semi-inverse method has been worked out for this purpose.

2. Isotropic plates

2.1. General relationships

A tensorial description of the theory of thin ideally plastic plates will now be presented as a convenient and general tool to deal with non-orthogonal situations. The cylindrical curvilinear coordinate system will be used

$$\begin{aligned} \eta^1&=\eta^1(x^1, x^2),\\ \eta^2&=\eta^2(x^1, x^2),\\ \eta^3&=x^3, \end{aligned} \tag{2.1}$$

where x^j, ($j=1, 2, 3$) are the Cartesian coordinates of generic points. The family η^3 constitutes straight lines paralled to x^3 and η^1, η^2, represent two families of plane curves as intersections of two families of cylindrical surfaces with the plane $x^3=$ $=\text{const}$ [22].

To consider an isotropic, rigid-perfectly plastic thin plate the postulated Huber–Mises yield condition must be expressed in the contravariant components of the symmetric tensor of moments $m^{\alpha\beta}$, $\alpha\beta=1, 2$ referred to the middle surface $x^3=\eta^3=0$. It assumes the form

$$F(m^{\alpha\beta})=m^{\alpha\gamma}m^{\beta\delta}(3g_{\beta\gamma}g_{\alpha\delta}-g_{\alpha\gamma}g_{\beta\delta})-m_0=0, \tag{2.2}$$

where $g_{\alpha\beta}$ stand for the components of the metric tensor

$$\begin{aligned} g_{\alpha\beta}&=\frac{\partial x^\gamma}{\partial\eta^\alpha}\frac{\partial x^\gamma}{\partial n^\beta},\\ \eta^\alpha&=\eta^\alpha(x^\beta). \end{aligned} \tag{2.3}$$

It should be noted that for isotropic and homogeneous plates m_0=const and for isotropic nonhomogeneous plates $m_0=m_0(\eta^1, \eta^2)$.

The flow rule associated with (2.2) can be written as

$$\dot{\kappa}_{\alpha\beta}=\dot{\lambda}\frac{\partial F}{\partial m^{\alpha\beta}}, \tag{2.4}$$

where

$$\frac{\partial F}{\partial m^{\alpha\beta}}=m^{\gamma\delta}(3g_{\gamma\beta}\,g_{\alpha\delta}-g_{\alpha\beta}\,g_{\gamma\delta})+m_{\varepsilon\eta}(3g_{\alpha\eta}\,g_{\varepsilon\beta}-g_{\varepsilon\eta}\,g_{\alpha\beta}).$$

Equilibrium of an element is expressed by the equation

$$m^{\alpha\beta}|_{\alpha\beta}=-p^3, \tag{2.5}$$

in which p^3 denotes the intensity of applied load acting downward.

Kinematical relations between the curvature rates and the deflection rates of the middle surface are as follows:

$$\dot{\kappa}_{\alpha\beta}=-\dot{w}|_{\alpha\beta}. \tag{2.6}$$

The vertical bar in Eqs. (2.5) and (2.6) implies covariant differentiation.

Shear forces can be expressed as

$$Q^{\alpha}=m^{\beta\alpha}|_{\alpha}, \tag{2.7}$$

and the Kirchhoff reactions along the edges are

$$V^{\alpha}=Q^{\alpha}+m^{\alpha\beta}|_{\beta}, \tag{2.8}$$

where $\alpha\neq\beta$ and no summation applies to β.

2.2. Relationships in the rectilinear skew coordinates

Let us assume a frame of reference η^k, $k=1, 2, 3$ such that

$$\begin{aligned}\eta^1&=x^1-x^2\operatorname{ctg}\alpha,\\ \eta^2&=x^2\frac{1}{\sin\alpha},\\ \eta^3&=x^3.\end{aligned} \tag{2.9}$$

Both coordinate systems x^j and η^k are shown in Fig. 1.

Remembering (2.3), the components of the metric tensor $g_{\alpha\beta}$ become:

$$g_{11}=1, \quad g_{12}=g_{21}=\cos\alpha, \quad g_{22}=1. \tag{2.10}$$

The yield condition (2.2) takes the form

$$F(m^{\alpha\beta})=(m^{11})^2+(m^{22})^2+(3+\cos^2\alpha)(m^{12})^2+ \\ +(3\cos^2\alpha-1)\,m^{11}\,m^{22}+4\cos\alpha\,(m^{11}+m^{22})\,m^{12}-m_0^2=0 \tag{2.11}$$

Such a representation in the contravariant components of the moment tensor does. not supply direct information on the distribution of "engineering" moments in the plate. Thus, let us rewrite (2.11) in the physical components $M^{\gamma\delta}$. These can be determined from [22]

$$M^{\gamma\delta}=m^{\alpha\beta}\left(\frac{g_{\beta\beta}}{g^{\alpha\alpha}}\right)^{\frac{1}{2}}\delta^{\gamma}_{\alpha}\,\delta^{\delta}_{\beta}, \tag{2.12}$$

where δ^{β}_{α} denotes the Kronecker delta.

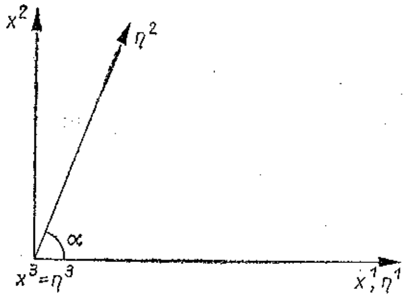

FIG. 1.

We obtain

$$M^{11}=m^{11}\sin\alpha,\qquad M^{12}=M^{21}=m^{12}\sin\alpha,\qquad M^{22}=m^{22}\sin\alpha \tag{2.13}$$

and the final form of (2.11) is

$$F(M^{\alpha\beta})=\frac{1}{\sin^2\alpha}\,[(M^{11})^2+(M^{22})^2+(3+\cos^2\alpha)\,(M^{12})^2+ \\ +(3\cos^2\alpha-1)\,M^{11}\,M^{22}+4\cos\alpha\,M^{12}\,(M^{11}+M^{22})]-m_0^2=0. \tag{2.14}$$

The moment tensor $m^{\alpha\beta}$ in the skew coordinates η^k is related to the moment tensor $\mathbf{m}^{\alpha\beta}$ in the Cartesian frame of reference x^α by the transformation rule [4]

$$m^{\alpha\beta}=\mathbf{m}^{\gamma\delta}\,\frac{\partial\eta^\alpha}{\partial x^\gamma}\,\frac{\partial\eta^\beta}{\partial x^\delta}. \tag{2.15}$$

All Greek indices run over 1, 2. Detailed calculation supplies:

$$\begin{aligned} m^{11}&=\mathbf{m}^{11}-2\mathrm{ctg}\,\alpha\mathbf{m}^{12}+\mathrm{ctg}^2\,\alpha\mathbf{m}^{22},\\ m^{12}&=m^{21}=\mathbf{m}^{12}\,\frac{1}{\sin\alpha}-\mathbf{m}^{22}\,\frac{\cos\alpha}{\sin^2\alpha},\\ m^{22}&=\mathbf{m}^{22}\,1\,\sin^2\alpha. \end{aligned} \tag{2.16}$$

On expressing $m^{\alpha\beta}$ in terms of the physical components $M^{\alpha\beta}$, see Eq. (2.13), and denoting, for brevity, that $\mathbf{m}^{11}=m_x$, $\mathbf{m}^{12}=\mathbf{m}^{21}=m_{xy}$, $\mathbf{m}^{22}=m_y$, we obtain the following form of Eq. (2.16):

$$\begin{aligned} M^{11}&=m_x\sin\alpha-2m_{xy}\cos\alpha+m_y\cos\alpha\,\mathrm{ctg}\,\alpha,\\ M^{12}&=M^{21}=m_{xy}-m_y\,\mathrm{ctg}\,\alpha,\\ M^{22}&=m_y\,\frac{1}{\sin\alpha}. \end{aligned} \tag{2.17}$$

The inverse formulae can be shown to be

$$
\begin{aligned}
m_x &= m^{11} + 2m^{12}\cos\alpha + m^{22}\cos^2\alpha,\\
m_{xy} &= m^{12}\sin\alpha + m^{22}\sin\alpha\cos\alpha,\\
m_y &= m^{22}\sin^2\alpha,
\end{aligned}
\tag{2.18}
$$

or, expressed in $M^{\alpha\beta}$ in place of $m^{\alpha\beta}$, become

$$
\begin{aligned}
m_x &= M^{11}\frac{1}{\sin\alpha} + 2M^{12}\operatorname{ctg}\alpha + M^{22}\cos\alpha\operatorname{ctg}\alpha,\\
m_{xy} &= M^{12} + M^{22}\cos\alpha,\\
m_y &= M^{22}\sin\alpha.
\end{aligned}
\tag{2.19}
$$

The relationships (2.17) and (2.19) were derived in [10] by cumbersome equilibrium considerations.

Similarly, the shear forces Q^α in the skew coordinates and $\mathbf{Q}^\alpha$ in the Cartesian coordinates obey the vectorial transformation rule

$$
Q^\alpha = \mathbf{Q}^\beta \frac{\partial \eta^\alpha}{\partial x^\beta}.
\tag{2.20}
$$

We obtain the following formulae:

$$
\begin{aligned}
Q^1 &= \mathbf{Q}^1 - \mathbf{Q}^2\operatorname{ctg}\alpha,\\
Q^2 &= \mathbf{Q}^2\frac{1}{\sin\alpha}.
\end{aligned}
\tag{2.21}
$$

Kinematical variables transform in a similar manner. Curvature rates $\dot{\kappa}_{\alpha\beta}$ in the rectilinear skew coordinates depend on those in the Cartesian coordinates as follows:

$$
\dot{\kappa}_{\alpha\beta} = \dot{\varkappa}_{\gamma\delta}\frac{\partial x^\gamma}{\partial \eta^\alpha}\frac{\partial x^\delta}{\partial \eta^\beta}.
\tag{2.22}
$$

It follows that:

$$
\begin{aligned}
\dot{\kappa}_{11} &= \dot{\varkappa}_{11},\\
\dot{\kappa}_{12} &= \dot{\kappa}_{21} = \dot{\varkappa}_{11}\cos\alpha + \dot{\varkappa}_{12}\sin\alpha,\\
\dot{\kappa}_{22} &= \dot{\varkappa}_{11}\cos^2\alpha + 2\dot{\varkappa}_{12}\sin\alpha\cos\alpha + \dot{\varkappa}_{22}\sin^2\alpha.
\end{aligned}
\tag{2.23}
$$

Denoting, for brevity, that $\dot{\varkappa}_{11} = \dot{\kappa}_x$, $\dot{\varkappa}_{22} = \dot{\kappa}_y$, $\dot{\varkappa}_{12} = (1/2)\,\dot{\kappa}_{xy}$ (since $\dot{\kappa}_{12} + \dot{\kappa}_{21} = \dot{\kappa}_{xy}$ and $\dot{\varkappa}_{\alpha\beta}$ is symmetric), Eq. (2.23) can be rewritten to be

$$
\begin{aligned}
\dot{\kappa}_{11} &= \dot{\kappa}_x,\\
2\dot{\kappa}_{12} &= 2\dot{\kappa}_x\cos\alpha + \dot{\kappa}_{xy}\sin\alpha,\\
\dot{\kappa}_{22} &= \dot{\kappa}_x\cos^2\alpha + \dot{\kappa}_{xy}\sin\alpha\cos\alpha + \dot{\kappa}_y\sin^2\alpha.
\end{aligned}
\tag{2.24}
$$

The inverse relations are as follows:

$$\dot{\kappa}_x = \dot{\kappa}_{11},$$
$$\dot{\kappa}_{xy} = -2\dot{\kappa}_{11} + 2\dot{\kappa}_{12}\frac{1}{\sin\alpha}, \tag{2.25}$$
$$\dot{\kappa}_y = \dot{\kappa}_{11}\operatorname{ctg}^2\alpha - \dot{\kappa}_{12}\operatorname{ctg}\alpha\frac{1}{\sin\alpha} + \dot{\kappa}_{22}\frac{1}{\sin^2\alpha}.$$

The associated flow law (2.4) takes, in the rectilinear skew frame of reference, the form:

$$\dot{\kappa}_{11} = \dot{\lambda}\,[2m^{11} + (3\cos^2\alpha - 1)\,m^{22} + 4\cos\alpha\, m^{12}],$$
$$\dot{\kappa}_{22} = \dot{\lambda}\,[2m^{22} + (3\cos^2\alpha - 1)\,m^{11} + 4\cos\alpha\, m^{12}], \tag{2.26}$$
$$\dot{\kappa}_{12} = \dot{\lambda}\,[2\cos\alpha\,(m^{11} + m^{22}) + (3 + \cos^2\alpha)\,m^{12}].$$

Alternatively, (2.26) can be expressed in terms of physical moment components $M^{\alpha\beta}$:

$$\dot{\kappa}_{11} = \frac{\dot{\lambda}}{\sin\alpha}\,[2M^{11} + (3\cos^2\alpha - 1)\,M^{22} + 4\cos\alpha\, M^{12}],$$
$$\dot{\kappa}_{22} = \frac{\dot{\lambda}}{\sin\alpha}\,[2M^{22} + (3\cos^2\alpha - 1)\,M^{11} + 4\cos\alpha\, M^{12}], \tag{2.27}$$
$$\dot{\kappa}_{12} = \frac{\dot{\lambda}}{\sin\alpha}\,[2\cos\alpha\,(M^{11} + M^{22}) + (3 + \cos^2\alpha)\,M^{12}].$$

The inverse form of (2.26) is:

$$m^{11} = \frac{1}{3\dot{\lambda}\sin^4\alpha}\,[2\dot{\kappa}_{11} + (1 + \cos^2\alpha)\,\dot{\kappa}_{22} - 4\cos\alpha\,\dot{\kappa}_{12}],$$
$$m^{22} = \frac{1}{3\dot{\lambda}\sin^4\alpha}\,[2\dot{\kappa}_{22} + (1 + \cos^2\alpha)\,\dot{\kappa}_{11} - 4\cos\alpha\,\dot{\kappa}_{12}], \tag{2.28}$$
$$m^{12} = \frac{1}{3\dot{\lambda}\sin^4\alpha}\,[-2\cos\alpha\,(\dot{\kappa}_{11} + \dot{\kappa}_{22}) + (1 + 3\cos^2\alpha)\,\dot{\kappa}_{12}].$$

Similarly, inversion of Eq. (2.27) furnishes

$$M^{11} = \frac{1}{3\dot{\lambda}\sin^3\alpha}\,[2\dot{\kappa}_{11} + (1 + \cos^2\alpha)\,\dot{\kappa}_{22} - 4\cos\alpha\,\dot{\kappa}_{12}],$$
$$M^{22} = \frac{1}{3\dot{\lambda}\sin^3\alpha}\,[2\dot{\kappa}_{22} + (1 + \cos^2\alpha)\,\dot{\kappa}_{11} - 4\cos\alpha\,\dot{\kappa}_{12}], \tag{2.29}$$
$$M^{12} = \frac{1}{3\dot{\lambda}\sin^3\alpha}\,[-2\cos\alpha\,(\dot{\kappa}_{11} + \dot{\kappa}_{22}) + (1 + 3\cos^2\alpha)\,\dot{\kappa}_{12}].$$

The equilibrium equation (2.5) in the skew situation becomes

$$m^{11}|_{11} + 2m^{12}|_{12} + m^{22}|_{22} = -p, \tag{2.30}$$

where, as before, the vertical bar denotes covariant differentiation.

Equation (2.30) in terms of physical moment components assumes the form

$$M^{11}|_{11}+2M^{12}|_{12}+M^{22}|_{22}=-p \sin \alpha \,. \tag{2.31}$$

The kinematical relations are

$$\dot{\kappa}_{\alpha\beta}=-\dot{w}|_{\alpha\beta} \,. \tag{2.32}$$

To formulate the statical boundary conditions it is necessary to derive formulae for the actual moments and forces acting on the edges of plates. By introducing additional orthogonal coordinates u, v (Fig. 2), we can express, for instance, the actual bending moment at the edge u=const (η^1=const) in the form

$$m_u=m_x \sin^2 \alpha+m_y \cos^2 \alpha-2m_{xy} \sin \alpha \cos \alpha \,. \tag{2.33}$$

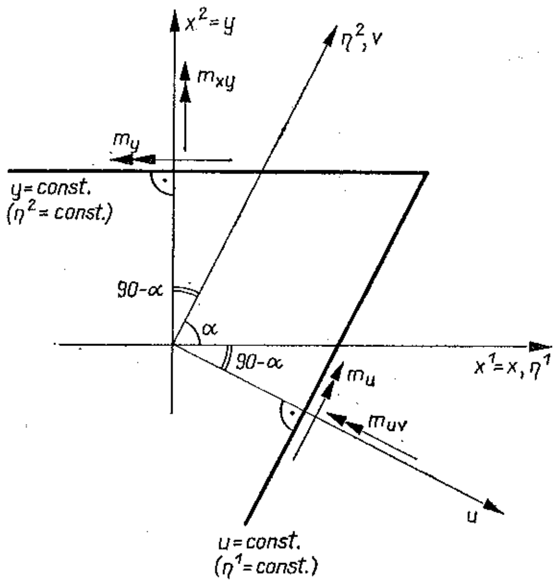

FIG. 2.

Comparison of Eq. (2.33) with Eq. (2.16) shows that

$$m_u=m^{11} \sin^2 \alpha=M^{11} \sin \alpha \,. \tag{2.34}$$

The actual twisting moment at the same edge has the magnitude

$$m_{uv}=\frac{1}{2}(m_x-m_y) \sin 2\alpha-m_{xy} \cos 2\alpha , \tag{2.35}$$

or, in terms of $m^{\alpha\beta}$ and $M^{\alpha\beta}$,

$$m_{uv}=m^{11} \cos \alpha \sin \alpha+m^{12} \sin \alpha=M^{11} \cos \alpha+M^{12}, \tag{2.36}$$

At the edge $y=\text{const}$ ($\eta^2=\text{const}$) we obtain the following actual moments:

$$m_y=m^{22}\sin^2\alpha=M^{22}\sin\alpha, \tag{2.37}$$

$$m_{xy}=m^{12}\sin\alpha+m^{22}\sin\alpha\cos\alpha=M^{12}+M^{22}\cos\alpha. \tag{2.38}$$

The actual Kirchhoff reactions are, cf. [10]:

$$\begin{aligned} V^1&=(m^{11}|_1+2m^{12}|_2)\sin\alpha \quad \text{for} \quad \eta^1=\text{const},\\ V^2&=(m^{22}|_2+2m^{12}|_1)\sin\alpha \quad \text{for} \quad \eta^2=\text{const}. \end{aligned} \tag{2.39}$$

The concentrated reactions at corners are, cf. [20]:

$$R=[m_{xy}+m_{uv}]_{\text{corner}}. \tag{2.40}$$

Equivalent forms are

$$\begin{aligned} R&=[2m^{12}\sin\alpha+(m^{11}+m^{22})\cos\alpha\sin\alpha]_{\text{corner}},\\ R&=[2M^{12}+(M^{11}+M^{22})\cos\alpha]_{\text{corner}}. \end{aligned} \tag{2.41}$$

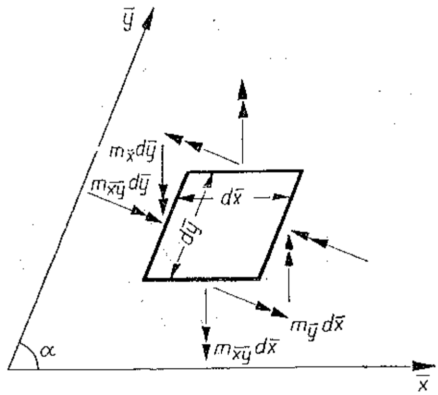

FIG. 3

In the specific applications to follow the simplified notation will be used, viz: the skew coordinates η^α will be replaced by $\bar{x}$, $\bar{y}$, the moments $m^{\alpha\beta}$ by $m_{\bar{x}}$, $m_{\bar{y}}$, $m_{\bar{x}\bar{y}}$, Fig. 3, the curvature rates $\dot{\kappa}_{\alpha\beta}$ will be denoted by $\dot{\kappa}_{11}=\dot{\kappa}_{\bar{x}}$, $\dot{\kappa}_{22}=\dot{\kappa}_{\bar{y}}$, $2\dot{\kappa}_{12}=\dot{\kappa}_{\bar{x}\bar{y}}$.

2.3. Complete solution of a nonhomogeneous parallelogram plate

A parallelogram plate resting on two pairs of edge beams with the lengths $2a$, $2b\leqslant 2a$, Fig. 4 will be conveniently described in the above introduced coordinates as well as statical and kinematical quantities.

The semi-inverse method of solution consists in assuming a moment distribution in the plate to within an accuracy of six constants. This distribution satisfies the hinge support conditions in the statical sense only. Then the curvature rate field is determined from the associated flow law and each of the curvature rates is suitably integrated to yield a field of deflection rates. Three versions of the relations are thus obtained and in each the corresponding coefficients are made equal. Simultaneous satisfaction of the kinematical boundary conditions will enable all the functions, all the integration constants and five, out of six, constants entering the assumed moment field to be found. The remaining constant will be determined from the plate equilibrium equation ensuring the unique bending and twisting moment distributions. A proper collapse mode will be found with deflections vanishing only at the corner supports of the structure.

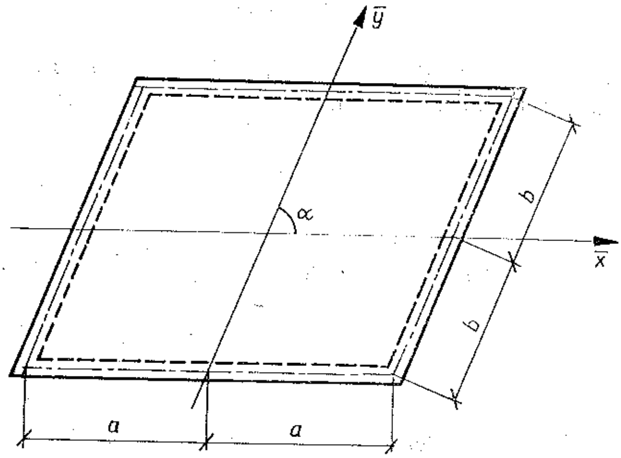

FIG. 4.

The moment field is assumed as follows:

$$m_{\bar{x}}=C_1(a^2-\bar{x}^2),$$
(2.42)
$$m_{\bar{y}}=C_4(b^2-\bar{y}^2),$$
$$m_{\bar{x}\bar{y}}=D_1\bar{x}^2+D_4\bar{y}^2+D_2\bar{x}\bar{y}+D_3ab.$$

Equations (2.26) supply the curvature rates:

(2.43) $$\dot{\kappa}_{\bar{x}}=\lambda\{\bar{x}^2(-2C_1+4\cos\alpha D_1)+[2C_1a^2+(3\cos^2\alpha-1)C_4b^2+ +4\cos\alpha D_3ab]+\bar{y}^2[(1-3\cos^2\alpha)C_4+4\cos\alpha D_4]+\bar{x}\bar{y}4\cos\alpha D_2\},$$

(2.44) $$\dot{\kappa}_{\bar{y}}=\lambda\{\bar{y}^2(-2C_4+4\cos\alpha D_4)+[2C_4b^2+(3\cos^2\alpha-1)C_1a^2+ +4\cos\alpha D_3ab]+\bar{x}^2[1-3\cos^2\alpha)C_1+4\cos\alpha D_1]+\bar{x}\bar{y}\cdot4\cos\alpha D_2\},$$

(2.45) $$\dot{\kappa}_{\bar{x}\bar{y}}=2\lambda\{\bar{x}^2[(3+\cos^2\alpha)D_1-2\cos\alpha C_1]+\bar{y}^2[(3+\cos^2\alpha)D_4- -2\cos\alpha C_4]+\bar{x}\bar{y}D_2(3+\cos^2\alpha)+[(3+\cos^2\alpha)D_3ab+ +2\cos\alpha C_1a^2+2\cos\alpha C_4b^2]\}.$$

Kinematical relations (2.6) take the explicit form

$$\dot{\kappa}_{\bar{x}} = -\frac{\partial^2 \dot{w}}{\partial \bar{x}^2}, \tag{2.46}$$

$$\dot{\kappa}_{\bar{y}} = -\frac{\partial^2 \dot{w}}{\partial \bar{y}^2}, \tag{2.47}$$

$$\dot{\kappa}_{\bar{x}\bar{y}} = -2\frac{\partial^2 \dot{w}}{\partial \bar{x}\,\partial \bar{y}}. \tag{2.48}$$

On equating the right-hand sides of Eqs. (2.43)–(2.45) and Eqs. (2.46)–(2.48) and suitably integrating, we obtain three versions of $\dot{w}(x, y)$:

$$\begin{aligned}\dot{w} = -\lambda \Big\{ & \frac{\bar{x}^4}{6}(-C_1 + 2\cos\alpha\, D_1) + \frac{\bar{x}^2}{2}[2C_1 a^2 + (3\cos^2\alpha - 1) C_4 b^2 + \\ & + 4\cos\alpha\, D_3 ab] + \frac{\bar{x}^2 \bar{y}^2}{2}[(1 - 3\cos^2\alpha) C_4 + 4\cos\alpha\, D_4] + \frac{\bar{x}^3 \bar{y}}{3} 2\cos\alpha\, D_2 + \\ & + f_1(\bar{y}) + g_1(\bar{y})\,\bar{x} + C\bar{x}\bar{y} + D \Big\},\end{aligned} \tag{2.49}$$

$$\begin{aligned}\dot{w} = -\lambda \Big\{ & \frac{\bar{y}^4}{6}(-C_4 + 2\cos\alpha\, D_4) + \frac{\bar{y}^2}{2}[2C_4 b^2 + (3\cos^2\alpha - 1) C_1 a^2 + \\ & + 4\cos\alpha\, D_3 ab] + \frac{\bar{x}^2 \bar{y}^2}{2}[(1 - 3\cos^2\alpha) C_1 + 4\cos\alpha\, D_1] + \\ & + \frac{\bar{x}\bar{y}^3}{3} 2\cos\alpha\, D_2 + f(\bar{x}) + g(\bar{x})\,\bar{y} + E\bar{x}\bar{y} + F \Big\},\end{aligned} \tag{2.50}$$

$$\begin{aligned}\dot{w} = -\lambda \Big\{ & \frac{\bar{x}^3 \bar{y}}{3}[(3 + \cos^2\alpha) D_1 - 2\cos\alpha\, C_1] + \frac{\bar{x}\bar{y}^3}{3}[(3 + \cos^2\alpha) D_4 - \\ & - 2\cos\alpha\, C_4] + \frac{\bar{x}^2 \bar{y}^2}{4} D_2 (3 + \cos^2\alpha) + \bar{x}\bar{y}[(3 + \cos^2\alpha) D_3 ab + \\ & + 2\cos\alpha\,(C_1 a^2 + C_4 b^2)] + h(\bar{x}) + h_1(\bar{y}) + G \Big\}.\end{aligned} \tag{2.51}$$

The following 11 functions and constants of integration enter the above expressions: $f_1(\bar{y})$, $g_1(\bar{x})$, C, D, $f(\bar{x})$, $g(\bar{x})$, E, F, $h(\bar{x})$, $h_1(\bar{y})$, G. Since the function of the deflection rate field must be unique, equating corresponding terms and using one kinematica lboundary conditions $\dot{w}(\pm a, \pm b) = 0$ supplies a set of equations from which all the functions and constants can be found to within an accuracy of one constant, for example C_1. Omitting tedious calculations and lengthy formulae, we shall show the final form of the deflection rate field constituting a proper mechanism of incipient plastic motion, Fig. 5.

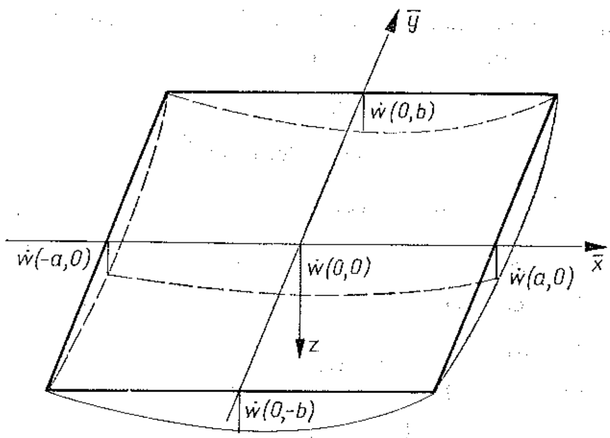

FIG. 5.

$$(2.52)\quad \dot{w}=\frac{\lambda C_1}{2(9-\cos^2\alpha)}\Big\{(\bar{x}^4+\bar{y}^4)(3-7\cos^2\alpha)-\bar{x}^2\bar{y}^2\cdot 3(1+\cos^2\alpha)(3+\cos^2\alpha)+$$
$$+\bar{x}^2\left[2a^2\frac{5\cos^4\alpha+38\cos^2\alpha-27}{3+\cos^2\alpha}+b^2\frac{3\cos^6\alpha-11\cos^4\alpha+13\cos^2\alpha+27}{3+\cos^2\alpha}\right]+$$
$$+\bar{y}^2\left[2b^2\frac{5\cos^4\alpha+38\cos^2\alpha-27}{3+\cos^2\alpha}+a^2\frac{3\cos^6\alpha-11\cos^4\alpha+13\cos^2\alpha+27}{3+\cos^2\alpha}\right]+$$
$$-[\bar{x}^3\bar{y}+\bar{x}\bar{y}^3-\bar{x}\bar{y}(a^2+b^2)]\cdot 8\cos\alpha(1+\cos^2\alpha)+$$
$$+\frac{(a^4+b^4)(45-58\cos^2\alpha-3\cos^4\alpha)+a^2b^2(-27+19\cos^2\alpha+43\cos^4\alpha-3\cos^6\alpha)}{3+\cos^2\alpha}\Big\}.$$

The deflection rate at the centre amounts to

$$(2.53)\quad \dot{w}(0,0)=\frac{\lambda C_1}{2(9-\cos^2\alpha)}\left[(a^4+b^4)\frac{45-58\cos^2\alpha-3\cos^4\alpha}{3+\cos^2\alpha}+\right.$$
$$\left.+a^2b^2\frac{-27+19\cos^2\alpha+43\cos^4\alpha-3\cos^6\alpha}{3+\cos^2\alpha}\right].$$

From the condition that the deflection at the midspan of the longer edge should not exceed that at the centre we obtain the equation $45-58\cos^2\alpha-3\cos^4\alpha>0$. Its solution imposes that $30°<\alpha\leqslant 90°$. Corresponding curvature rates can be computed from Eqs. (2.43)–(2.45).

The moment field (2.42) now becomes

$$m_{\bar{x}}=C_1(a^2-\bar{x}^2),$$
$$m_{\bar{y}}=C_1(b^2-\bar{y}^2),$$
$$(2.54)\quad m_{\bar{x}\bar{y}}=\frac{C_1}{9-\cos^2\alpha}\left[(\bar{x}^2+\bar{y}^2)\,10\cos\alpha+\bar{x}\bar{y}\cdot 6(1+\cos^2\alpha)-\right.$$
$$\left.-a^2b^2\frac{2\cos\alpha(1+\cos^2\alpha)}{3+\cos^2\alpha}\right].$$

The plate equilibrium equation (2.30) enables the remaining constant C_1 to be related to the applied load p. We obtain

$$C_1 = \frac{9-\cos^2\alpha}{8(3-2\cos^2\alpha)}\, p. \tag{2.55}$$

The moment field eventually becomes

$$\begin{aligned} m_{\bar{x}} &= \frac{9-\cos^2\alpha}{8(3-2\cos^2\alpha)}\, p\,(a^2-\bar{x}^2),\\ m_{\bar{y}} &= \frac{9-\cos^2\alpha}{8(3-2\cos^2\alpha)}\, p\,(b^2-\bar{y}^2),\\ m_{\bar{x}\bar{y}} &= \frac{1}{4(3-2\cos^2\alpha)}\, p\left[(\bar{x}^2+\bar{y}^2)\,5\cos\alpha+3\bar{x}\bar{y}\,(1+\cos^2\alpha)-\right.\\ &\qquad\left.-(a^2+b^2)\frac{\cos\alpha\,(1+\cos^2\alpha)}{3+\cos^2\alpha}\right]. \end{aligned} \tag{2.56}$$

The edge reactions are

$$\begin{aligned} V_{\bar{x}} &= \frac{p\sin\alpha}{4(3-2\cos^2\alpha)}\,[\pm(7\cos^2\alpha-3)\,a+20\cos\alpha\,\bar{y}] \quad \text{for} \quad \bar{x}=\pm a,\\ V_{\bar{y}} &= \frac{p\sin\alpha}{4(3-2\cos^2\alpha)}\,[\pm(7\cos^2\alpha-3)\,b+20\cos\alpha\,\bar{x}] \quad \text{for} \quad \bar{y}=\pm b. \end{aligned} \tag{2.57}$$

The corner reactions can be calculated from the formula

$$R = [2m_{\bar{x}\bar{y}}+(m_{\bar{x}}+m_{\bar{y}})\cos\alpha]\sin\alpha|_{\text{corner}} \tag{2.58}$$

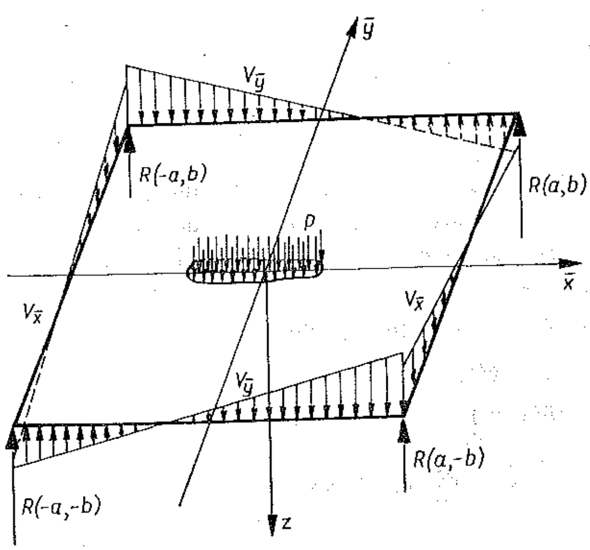

FIG. 6.

and have the values

$$R = \frac{p \sin\alpha\,(1+\cos^2\alpha)}{2\,(3-2\cos^2\alpha)}\left[\frac{4\cos\alpha}{3+\cos^2\alpha}\,(a^2+b^2)+3ab\right] \quad \text{for} \quad \bar{x}=\pm a, \quad \bar{y}=\pm b,$$

(2.59)

$$R = \frac{p \sin\alpha\,(1+\cos^2\alpha)}{2\,(3-2\cos^2\alpha)}\left[\frac{4\cos\alpha}{3+\cos^2\alpha}\,(a^2+b^2)-3ab\right] \quad \text{for} \quad \bar{x}=\pm a, \quad \bar{y}=\mp b.$$

All active and reactive loads are shown in Fig. 6. As a check on all the above shown results the global equilibrium of the system as well as the virtual work equation $D_{ext}=D_{int}$ were written down and found to be satisfied in an exact manner.

Lastly, let us determine explicitly the plastic nonhomogeneity of the considered isotropic plate. Substitution of Eq. (2.56) into the yield condition (2.11) gives the ultimate bending moment as a function of $\bar{x}$, $\bar{y}$:

(2.60)
$$\begin{aligned} m_0(\bar{x},\bar{y}) = \frac{p}{4\,(3-2\cos^2\alpha)} \Bigg[& (a^4+b^4)\frac{243-281\cos^2\alpha+89\cos^4\alpha+13\cos^6\alpha}{4\,(3+\cos^2\alpha)} + \\ & + a^2 b^2 \frac{-243+86\cos^2\alpha+304\cos^4\alpha-22\cos^6\alpha+3\cos^8\alpha}{4\,(3+\cos^2\alpha)} + \\ & + (\bar{x}^4+\bar{y}^4)\frac{3}{4}(27-26\cos^2\alpha+47\cos^4\alpha) + \\ & + \bar{x}^2\bar{y}^2\frac{3}{4}(9+131\cos^2\alpha+135\cos^4\alpha+13\cos^6\alpha) + \\ & + (\bar{x}^3\bar{y}+\bar{x}\bar{y}^3)\,36\cos\alpha\,(1+\cos^2\alpha) + \bar{x}\bar{y}\,(a^2+b^2)\,(-12\cos\alpha)\,(1+\cos^2\alpha)^2 + \\ & + \bar{x}^2\left(a^2\frac{-486+489\cos^2\alpha-306\cos^4\alpha-90\cos^6\alpha}{3+\cos^2\alpha} + \right. \\ & \left. + b^2\frac{243-150\cos^2\alpha-432\cos^4\alpha-42\cos^6\alpha-3\cos^8\alpha}{3+\cos^2\alpha}\right) + \\ & + \bar{y}^2\left(b^2\frac{-486+489\cos^2\alpha-306\cos^4\alpha-90\cos^6\alpha}{3+\cos^2\alpha} + \right. \\ & \left. + a^2\frac{243-150\cos^2\alpha-432\cos^4\alpha-42\cos^6\alpha-3\cos^8\alpha}{3+\cos^2\alpha}\right)\Bigg]^{\frac{1}{2}}. \end{aligned}$$

This function leads to the exact plastic design of two practical types of plate-beam systems:

a) Reinforced plate with constant thickness. The function (2.60) ensuring the simultaneous onset of yielding in the whole plate should be reproduced as closely as possible by varying intensity of reinforcement.

b) Plate of homogenenous material. The function (2.60) supplies the variation of thickness according to the rule

$$h(\bar{x}, \bar{y}) = 2\sqrt{\frac{m_0(\bar{x}, \bar{y})}{\sigma_0}}, \tag{2.61}$$

where σ_0 is the yield point of the material. Thickness at the centre will be

$$h(0,0) = \left[\frac{p}{\sigma_0(3-2\cos^2\alpha)}\right]^{\frac{1}{2}} \left[(a^4+b^4)\frac{243-281\cos^2\alpha+89\cos^4\alpha+13\cos^6\alpha}{3+\cos^2\alpha} + \right.$$
$$\left. + a^2 b^2 \frac{-243+86\cos^2\alpha+304\cos^4\alpha-22\cos^6\alpha+3\cos^8\alpha}{3+\cos^2\alpha}\right]^{\frac{1}{2}}. \tag{2.62}$$

Plastic bending moments in edge beams follow from Eq. (2.60) and to ensure yielding simultaneously with the plate, have the following distributions:

$$\begin{aligned} m_b(\bar{x}) &= \frac{p}{8(3-2\cos^2\alpha)}\left[(3-7\cos^2\alpha)\, b\,(a^2-\bar{x}^2) - \frac{20\cos\alpha}{3}(a^2\bar{x}-\bar{x}^3)\right], \\ m_b(\bar{y}) &= \frac{p}{8(3-2\cos^2\alpha)}\left[(3-7\cos^2\alpha)\, a\,(b^2-\bar{y}^2) - \frac{20\cos\alpha}{3}(b^2\bar{y}-\bar{y}^3)\right]. \end{aligned} \tag{2.63}$$

The function (2.60) was programmed to supply a number of thickness distributions for various ratios of $b/a \leqslant 1$ and various angles α. Figure 7 shows the variation of thickness for $b/a=0.8$, $\alpha=70°$.

Specific systems encountered in engineering practice can be readily derived from the above solution:

1) a rhombus system, $a=b$,
2) a rectangular system, $\alpha=90°$,
3) a square system, $a=b$, $\alpha=90°$.

Let us present the results for the rectangular system. The field of deflection rates assumes the form ($\bar{x}=x$, $\bar{y}=y$):

$$\dot{w}(x,y) = \dot{A}_1\left[x^4+y^4-3(2a^2-b^2)x^2-3(2b^2-a^2)y^2 + \right.$$
$$\left. -3x^2y^2+5(a^4+b^4)-3a^2b^2\right]. \tag{2.64}$$

The associated curvature rates are

$$\begin{aligned} \dot{\kappa}_x &= -6\dot{A}_1(2x^2-2a^2-y^2+b^2), \\ \dot{\kappa}_y &= -6\dot{A}_1(2y^2-2b^2-x^2+a^2), \\ \dot{\kappa}_{xy} &= 24\dot{A}_1\, xy. \end{aligned} \tag{2.65}$$

It is worth emphasizing that the field (2.64) resulting formally from (2.52) can be directly interpreted as the following sum:

$$\dot{w}(x,y) = \dot{w}_b(x) + w_b(y) + f_1(x,y), \tag{2.66}$$

where the first two terms represent the deflection rates of edges and the function $f(x, y)$ must vanish there as well as remain doubly symmetrical and satisfy the statical boundary conditions. It turns out that the deflection rates at the edges can

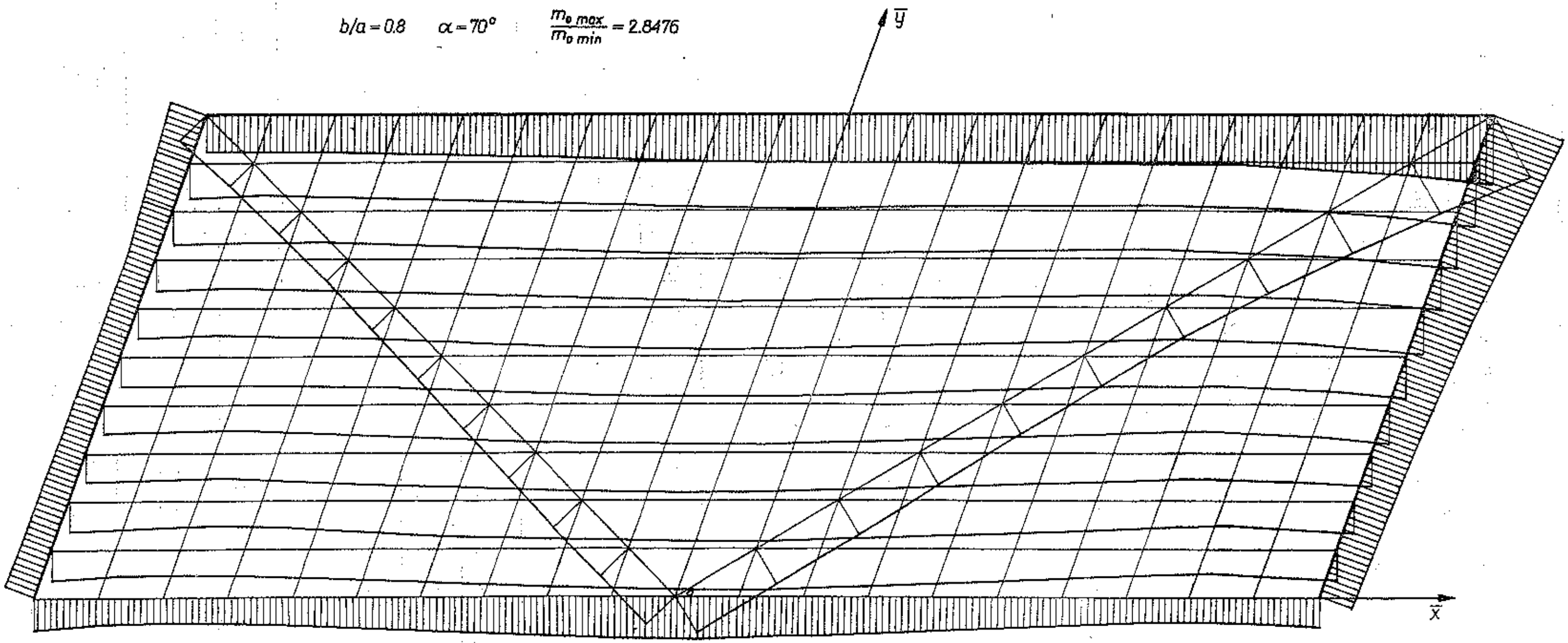

FIG. 7.

be taken as proportional to the elastic deflections of simple beams under uniformly distributed load, that is, for instance, $w_b(x)=\dot{A}_1(x^4-6a^2x^2+5a^4)$. Then the third term in Eq. (2.66) assumes the form $f_1(x,y)=-3\dot{A}_1(a^2-x^2)(b^2-y^2)$.

The moment field is described by

$$
\begin{aligned}
m_x &= \frac{3}{8}p(a^2-x^2),\\
m_y &= \frac{3}{8}p(b^2-y^2),\\
m_{xy} &= \frac{1}{4}pxy,
\end{aligned}
\tag{2.67}
$$

the edge reactions are uniform,

$$
\begin{aligned}
V_x &= \mp\frac{1}{4}pa \quad \text{for} \quad x=\pm a,\\
V_y &= \mp\frac{1}{4}pb \quad \text{for} \quad y=\pm b
\end{aligned}
\tag{2.68}
$$

and the corner reactions are $R=pab/2$ each.

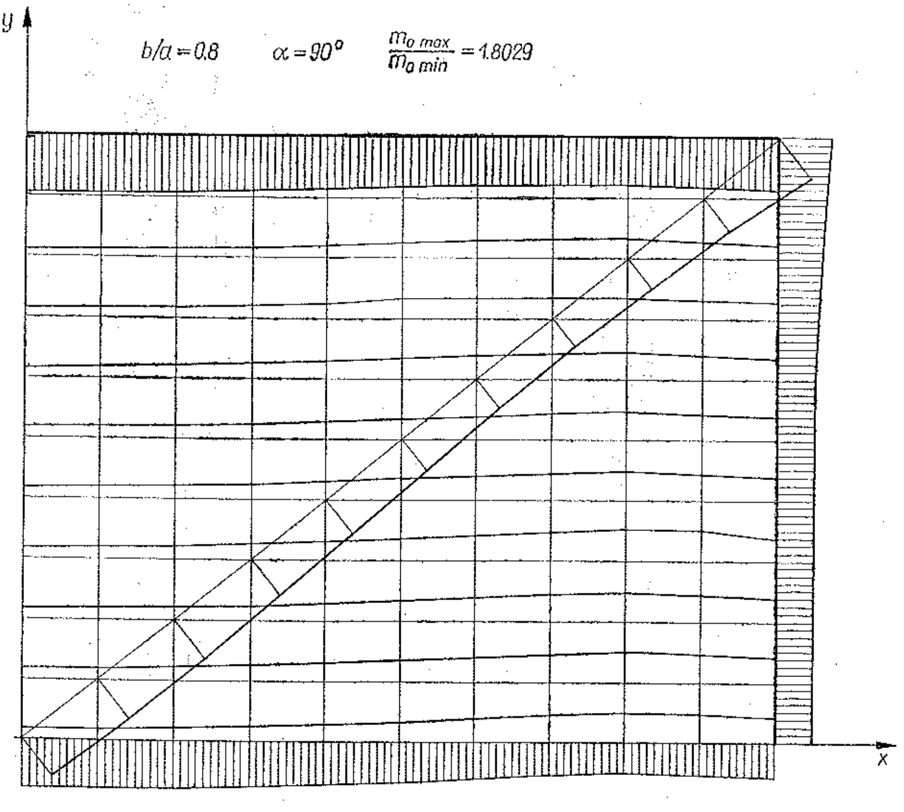

FIG. 8.

The variation of thickness should obey the function

$$h(x, y)=\left(\frac{3p}{2\sigma_0}\right)^{\frac{1}{2}} [x^4+y^4+a^4+b^4-a^2 b^2+(b^2-2a^2) x^2+ +(a^2-2b^2) y^2+(1/3) x^2 y^2]^{\frac{1}{4}} \tag{2.69}$$

and the thickness at the centre is

$$h(0, 0)=\left(\frac{3p}{2\sigma_0}\right)^{\frac{1}{2}} (a^4+b^4-a^2 b^2)^{\frac{1}{4}}. \tag{2.70}$$

Variations of thickness for $b/a=0{,}8$ and 1 are shown in Figs. 8 and 9.

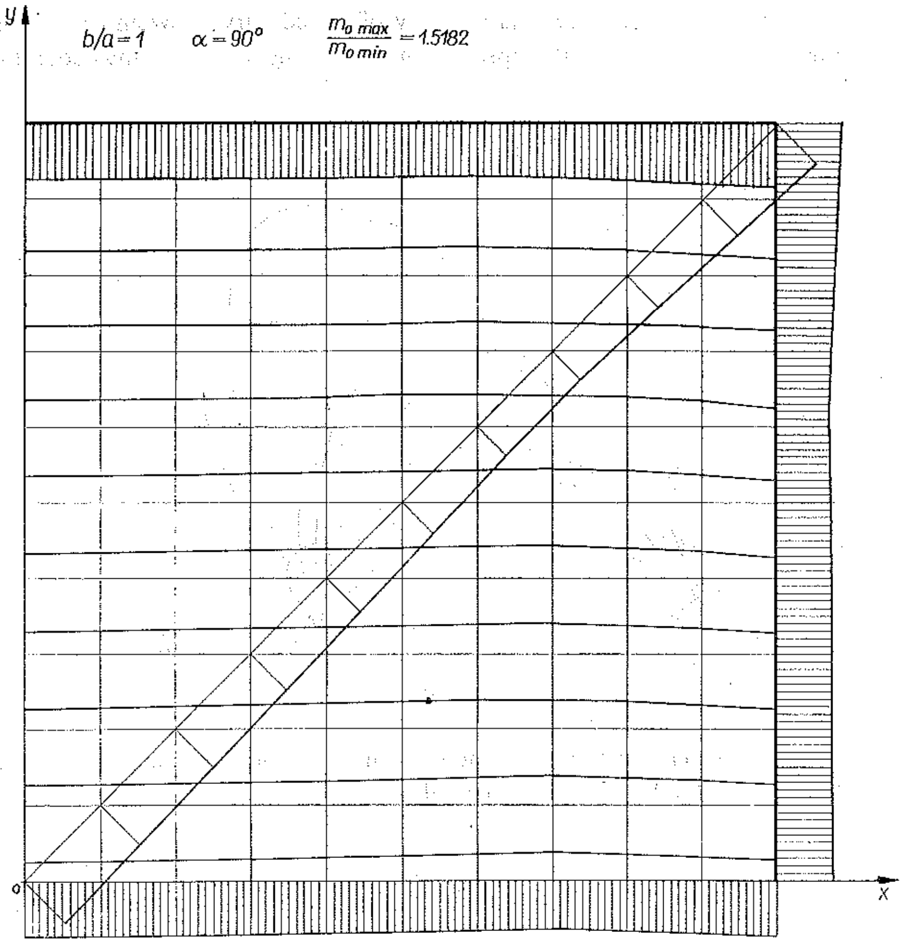

FIG. 9.

3. ORTHOTROPIC PLATES

In many situations a special type of anisotropy, viz. orthotropy, is of technical importance. Here belong plates reinforced in two perpendicular directions, densely ribbed plates and so on. It is therefore of interest to derive all the necessary relationships for orthotropic plastic plates.

3.1. General relationships

Let us confine ourselves to structures consisting of rectangular plates and two pairs of orthogonal edge beams. The modified Huber–Mises yield condition will be expressed in the Cartesian coordinate system [19]

$$F = m_1^2 - 2dm_1 m_2 + e^2 m_2^2 - m_0^2(x, y) = 0, \tag{3.1}$$

where m_1, m_2 denote the principal bending moments, $m_0(x, y)$ stands for the ultimate bending moment in the section x=const of a nonhomogeneous plate and d, e are constants which should ideally be determined from experiments on a plate in question. Equation (3.1) represents a family of closed curves. When $e^2 > d^2$, the curves constitute a family of real ellipses as shown in Fig. 10 for various combinations of e and d.

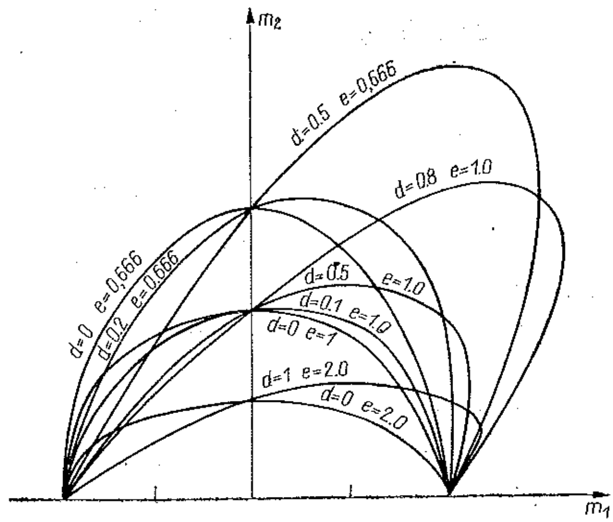

FIG. 10.

The condition (3.1) will now be expressed in terms of moments m_x, m_y, m_{xy}. Having the standard transformation formulae

$$\begin{aligned} m_1 &= \frac{1}{2}(m_x + m_y) + \frac{1}{2}[(m_x - m_y)^2 + 4m_{xy}^2]^{\frac{1}{2}}, \\ m_2 &= \frac{1}{2}(m_x + m_y) - \frac{1}{2}[(m_x - m_y)^2 + 4m_{xy}^2]^{\frac{1}{2}}, \end{aligned} \tag{3.2}$$

we obtain, after rearranging, the following form of the yield condition for nonhomogeneous orthotropic plates:

$$\begin{aligned} F = \frac{1}{2}(1+e^2)(m_x^2 + m_y^2) + \frac{1}{2}(1-e^2)(m_x + m_y)[(m_x - m_y)^2 + 4m_{xy}^2]^{\frac{1}{2}} - \\ - 2dm_x m_y + (1 + 2d + e^2) m_{xy}^2 - m_0^2(x, y) = 0. \end{aligned} \tag{3.3}$$

It can readily be seen that for $d=0.5$, $e=1$ we obtain the well known Huber–Mises yield condition for isotropic plates.

Bearing in mind the explicit form of the associated flow law

$$
\begin{aligned}
\dot{\kappa}_x &= \lambda \frac{\partial F}{\partial m_x}, \\
\dot{\kappa}_y &= \lambda \frac{\partial F}{\partial m_y}, \qquad (3.4)\\
\dot{\kappa}_{xy} &= \lambda \frac{\partial F}{\partial m_{xy}},
\end{aligned}
$$

performing on Eq. (3.3) the necessary differentiation and rearranging, we get the relationships between the curvature rates and moments:

$$
\begin{aligned}
\dot{\kappa}_x &= \lambda \left\{ (1+e^2)\, m_x - 2dm_y + (1-e^2) \frac{m_x^2 - m_x m_y + 2m_{xy}^2}{[(m_x-m_y)^2+4m_{xy}]^{\frac{1}{2}}} \right\}, \\
\dot{\kappa}_y &= \lambda \left\{ (1+e^2)\, m_y - 2dm_x + (1-e^2) \frac{m_y^2 - m_x m_y + 2m_{xy}^2}{[(m_x-m_y)^2+4m_{xy}^2]^{\frac{1}{2}}} \right\}, \qquad (3.5)\\
\dot{\kappa}_{xy} &= \lambda \left\{ (1+2d+e^2) + (1-e^2) \frac{m_x+m_y}{[(m_x-m_y)^2+4m_{xy}^2]^{\frac{1}{2}}} \right\} 2m_{xy}.
\end{aligned}
$$

Inserting (3.5), we arrive at the required formulae

$$
\begin{aligned}
m_x &= \frac{1}{8\lambda\,(e^2-d^2)} \left\{ 2\,(1+e^2)\, \dot{\kappa}_x + 4d\dot{\kappa}_y - (1-e^2) \frac{2\dot{\kappa}_x^2 - 2\dot{\kappa}_x \dot{\kappa}_y + \dot{\kappa}_{xy}^2}{[(\dot{\kappa}_x-\dot{\kappa}_y)^2+\dot{\kappa}_{xy}^2]^{\frac{1}{2}}} \right\}, \\
m_y &= \frac{1}{8\lambda\,(e^2-d^2)} \left\{ 2\,(1+e^2)\, \dot{\kappa}_y + 4d\dot{\kappa}_x - (1-e^2) \frac{2\dot{\kappa}_y^2 - 2\dot{\kappa}_x \dot{\kappa}_y + \dot{\kappa}_{xy}^2}{[(\dot{\kappa}_x-\dot{\kappa}_y)^2+\dot{\kappa}_{vy}^2]^{\frac{1}{2}}} \right\}, \qquad (3.6)\\
m_{xy} &= \frac{1}{8\lambda\,(e^2-a^2)} \left\{ (1-2d+e^2) - (1-e^2) \frac{\dot{\kappa}_x+\dot{\kappa}_y}{[(\dot{\kappa}_x-\dot{\kappa}_y)^2+\dot{\kappa}_{xy}^2]^{\frac{1}{2}}} \right\} \dot{\kappa}_{xy}.
\end{aligned}
$$

The plate equilibrium equation can be written as

$$
m_{x,xx} + 2m_{xy,xy} + m_{y,yy} = -p. \qquad (3.7)
$$

The kinematical relations are

$$
\begin{aligned}
\dot{\kappa}_x &= -\dot{w}_{,xx}, \\
\dot{\kappa}_y &= -\dot{w}_{,yy}, \qquad (3.8)\\
\dot{\kappa}_{xy} &= -2\dot{w}_{,xy}.
\end{aligned}
$$

Thus, we have the complete set of 8 equations (3.3), (3.6), (3.7) and (3.8) in 8 unknown functions m_x, m_y, m_{xy}, $\dot{\kappa}_x$, $\dot{\kappa}_y$, $\dot{\kappa}_{xy}$, $\dot{w}$, λ. The formulae for edge reactions and corner forces are

$$
\begin{aligned}
V_x &= m_{x,x} + 2m_{xy,y}, \\
V_y &= m_{y,y} + 2m_{xy,x}, \qquad (3.9)\\
R &= 2m_{xy}.
\end{aligned}
$$

The Huber–Mises yield condition for nonhomogeneous orthotropic plates and the associated flow law have also been derived in the rectilinear skew coordinate system. However, since no examples of parallelogram orthotropic plates have yet been worked out, the relevant equations will not be shown in the paper.

3.2. Rectangular orthotropic plate

A rectangular plate with the sides $2a\times 2b$, $b\leqslant a$, is considered resting on sinking edge beams. The whole system is point-supported at the corners.

The field of deflection rates is assumed as a sum of deflection rates each proportional to the elastic deflections of neighbouring edge beams,

$$\dot{w}=\dot{w}_b(x)+\dot{w}_b(y), \tag{3.10}$$

where

$$\begin{aligned} \dot{w}_b(x)&=\dot{D}\,(x^4-6a^2x^2+5a^4),\\ \dot{w}_b(y)&=\dot{D}\,(y^4-6b^2y^2+5b^4). \end{aligned} \tag{3.11}$$

It should be emphasized that the common coefficient D in both expressions (3.11) imposes no constraints on the solution sought. The kinematically admissible field of deflection rates is shown in Fig. 11. Making use of Eqs. (3.11) and (3.8) we get

$$\begin{aligned} \dot{\kappa}_x&=12\dot{D}\,(a^2-x^2),\\ \dot{\kappa}_y&=12\dot{D}\,(b^2-y^2),\\ \dot{\kappa}_{xy}&=0. \end{aligned} \tag{3.12}$$

Vanishing $\dot{\kappa}_{xy}$ results in the fact that the nonlinear relationships (3.6) now become linear. In fact, we obtain

$$\begin{aligned} m_x&=\frac{1}{2\lambda\,(e^2-d^2)}\,(e^2\,\dot{\kappa}_x+d^2\,\dot{\kappa}_y),\\ m_y&=\frac{1}{2\lambda\,(e^2-d^2)}\,(e^2\,\dot{\kappa}_y+d^2\,\dot{\kappa}_x),\\ m_{xy}&=0. \end{aligned} \tag{3.13}$$

No torsional action is supported by the plate deforming according to Eq. (3.10). Inserting Eq. (3.12) into Eq. (3.13), we obtain the following distribution of bending moments:

$$\begin{aligned} m_x&=\frac{6\dot{D}}{\lambda\,(e^2-d^2)}\,[e^2\,(a^2-x^2)+d\,(b^2-y^2)],\\ m_y&=\frac{6\dot{D}}{\lambda\,(e^2-d^2)}\,[e^2\,(b^2-y^2)+d\,(a^2-x^2)],\\ m_{xy}&=0. \end{aligned} \tag{3.14}$$

The statical boundary conditions

$$m_x(\pm a)=0, \quad m_y(\pm b)=0 \tag{3.15}$$

can only be satisfied for $d=0$. This means that the ellipses in Fig. 9 must be symmetrical with respect to the m_2 (or m_1)-axis. Making use of the plate equilibrium equation (3.7) in the case of uniformly distributed load, we find that

$$\frac{\dot{D}}{\lambda}=\frac{pe^2}{12(1+e^2)}. \tag{3.16}$$

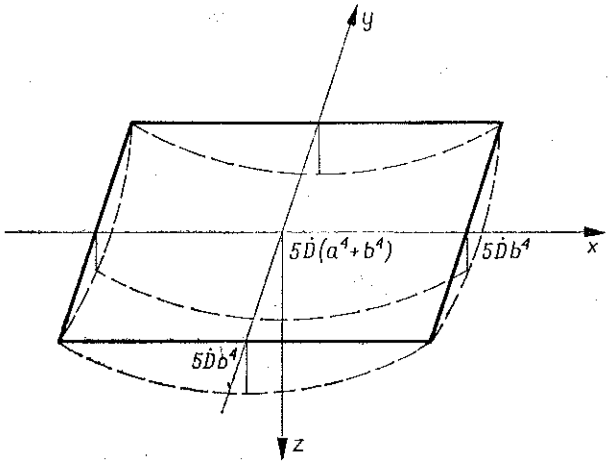

FIG. 11.

The bending moment distribution attains the final form

$$m_x=\frac{pe^2}{2(1+e^2)}(a^2-x^2), \quad m_y=\frac{p}{2(1+e^2)}(b^2-y^2), \quad m_{xy}=0. \tag{3.17}$$

Edge reactions are

$$V_x(\pm a)=\pm\frac{pae^2}{1+e^2}, \quad V_y(\pm b)=\pm\frac{pb}{1+e^2}, \tag{3.18}$$

whereas the corner force vanishes due to the absence of twisting moments. It can easily be shown that both the global equilibrium and the virtual work equation are satisfied in an exact manner.

The design of the plate should ensure the simultaneous yielding of the whole structure at the ultimate load p. On inserting Eq. (3.17) into Eq. (3.1) and remembering that $d=0$, and $m_1=m_x$, $m_2=m_y$, we finally obtain the ultimate bending moment m_0 as a function of x, y:

$$(3.19)\qquad m_0(x,y)=\frac{pe}{2(1+e^2)}\left[e^2x^4+y^4-2(e^2a^2x^2+b^2y^2)+e^2a^4+b^4\right]^{\frac{1}{2}}.$$

Introducing the so-called coefficient of orthotropy $k(x, y)$ we have, on account of (3.17),

$$(3.20)\qquad k(x,y)=\frac{m_x}{m_y}=e^2\frac{a^2-x^2}{b^2-y^2}.$$

Orthotropy at the centre of the plate is characterized by

$$(3.21)\qquad k_c=e^2\frac{a^2}{b^2},\qquad m_{0c}=\frac{pe}{2(1+e^2)}(e^2a^4+b^4)^{\frac{1}{2}}.$$

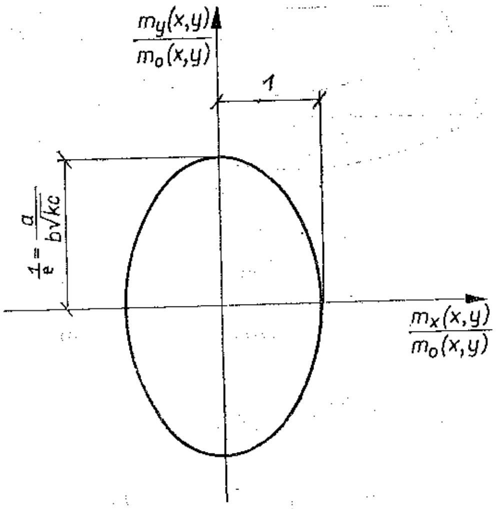

FIG. 12.

The relevant yield condition for a generic point x, y is depicted in Fig. 12 in the plane of dimensionless bending moments. The formula (3.20) gives the mechanical meaning to the coefficient e introduced in Eq. (3.1).

The distribution of ultimate bending moments in the edge beams must be as follows:

$$(3.22)\qquad m_b(x)=\frac{pb}{2(1+e^2)}(a^2-x^2),\qquad m_b(y)=\frac{pae^2}{2(1+e^2)}(b^2-y^2).$$

It should be borne in mind that the above solution does not tend to the limiting case of isotropy because two strong assumptions have been made: $\dot{\kappa}_{xy}=0$, which enabled the associated flow law to be linearized and $d=0$, which satisfied the statical boundary conditions but confined the class of plates to those obeying the yield condition as shown in Fig. 12. It is therefore of little interest to show a specific case of a square orthogonal plate unless some external requirements are imposed to insist on orthotropy.

No polynomial closed form solutions to the orthotropic plates supporting torsion, i.e. for the nonlinear relationships between moments and curvature rates, have been found.

References

1. J. F. Collins, *On an analogy between plane strain and plate bending solution in rigid/perfect plasticity theory*, Int. J. Solid Struct., 7, 1053–1057, 1971.
2. M. J. Estrin, *Plastic bending of rigid-perfectly plastic plates* [in Russian], Iss. po stroit. mech., Gosstrojddat, 67–74, Moscow 1962,
3. E. N. Fox, *Limit analysis for plates: a simple loading problem involving a complex exact solution*, A. Mat. and Physical Sci., 272, 463–492, 1972.
4. G. A. Hawkins, *Multilinear analysis for students in engineering and science*, John Wiley and Sons Inc., New York and London 1963.
5. P. G. Hodge Jr., *Plastic analysis of structures*, McGraw–Hill, New York 1959.
6. H. G. Hopkins, *On the plastic theory of plates*, Proceedings of the Royal Society of London, Ser. A. 241, 153–179, 1957.
7. M. Kwieciński, *Plastic exhaustion of the load-carrying capacity of ribbed plates. Kinematical solutions* [in Polish], Rozpr. Inżyn., **11**, 2, 1963.
8. M. Kwieciński, *Plastic exhaustion of the load-carrying capacity of ribbed plates. Statical solutions* [in Polish], Rozpr. Inż., **11**, 3, 1963.
9. M. Kwieciński, *Ultimate load of reinforced concrete slab-beam system* [in Polish], Arch. Inż. Lądow. **25**, 4, 1979.
10. L. S. D. Morley, *Skew plates and structures*, Pergamon Press, Oxford, London, New York, Paris 1963.
11. M. P. Nielsen, *Limit analysis of reinforced concrete slabs*, Acta Polytechnica Scandinavica, Oi 26, Copenhagen 1964.
12. D. Niepostyn, *Load-bearing capacity of axisymmetric plates* [in Polish], Arkady, Warszawa 1963.
13. A. Sawczuk, P. G. Hodge Jr., *Limit analysis and yield line theory*, J. App. Mech., **35**, 357–362, 1968.
14. A. Sawczuk, J. Sokół–Supel, *Bending of plates obeying maximum principal moment yield criterion*, Bull. Acad. Polon. Sci., Sérié Sci. Techn., **23**, 141–150, 1975.
15. W. S. Schumann, *On limit analysis of plates*, Quart. Of Appl. Math., **16**, 61–71, 1958.
16. Z. Sobotka, *Load-bearing capacity of plates* [in Polish], Arkady, Warszawa 1975.
17. J. Sokół–Supel, *Discontinuous stress field in plastic plates at collapse under distributed load*, Bull. Acad. Polon. Sci., Série Sci. Techn., **23**, 4, 1975.
18. J. Sokół–Supel, *Semi-inverse method to obtain complete solutions to the load-bearing capacity of plates* [in Polish], Rozpr. Inż., **24**, 4, 797–807, 1976.
19. J. Sokół–Supel, *Numerical method for evaluation of bearing capacity of axisymmetric plates*, Rozpr. Inż., **26**, 1, 179–191, 1978.

20. W. Wojewódzki, M. Kwieciński, *Ultimate load of orthotropic skew plate* [in Polish], Arch. Inż. Ląd., 14, 2, 1968.
21. R. N. Wood, *Plastic and elastic design of slabs and plates*, London, Thames and Hudson, 1961.
22. J. Zawidzki, *Plane plasticity in nonorthogonal coordinate systems* [in Polish], Rozpr. Inż., 15, 4, 1967.

STRESZCZENIE

ROZWIĄZANIA ZUPEŁNE NIEJEDNORODNYCH PŁYT PLASTYCZNYCH OPARTYCH NA PODATNYCH ŻEBRACH

W pracy przedstawiono metodę półodwrotną otrzymywania rozwiązań zupełnych cienkich niejednorodnych płyt plastycznych opartych na żebrach, które uginają się razem z brzegami płyty. Płyty i żebra uplastyczniają się zgodnie z warunkiem Hubera–Misesa i podlegają stowarzyszonemu prawu płynięcia. Ustrój jest obciążony poprzecznie obciążeniem równomiernym i podparty w narożach. Uzyskano rozwiązania zupełne dla płyt izotropowych w kształcie kwadratu, prostokąta, rombu i równoległoboku. Rozważono również kwadratowe i prostokątne płyty ortotropowe. Otrzymane rozwiązania umożliwiają projektowanie płyt niejednorodnych, przy czym zaprojektowana niejednorodność gwarantuje pełne uplastycznienie całej konstrukcji w chwili wyczerpania nośności. Opracowany został opis teorii cienkich płyt plastycznych, podlegających warunkowi Hubera–Misesa w nieortogonalnym układzie współrzędnych krzywoliniowych. Następnie wyspecyfikowano ten opis dla ukośnokątnego układu współrzędnych prostoliniowych, stwarzając dogodne narzędzie do rozwiązywania płyt równoległobocznych.

Резюме

ПОЛНЫЕ РЕШЕНИЯ НЕОДНОРОДНЫХ ПЛАСТИЧЕСКИХ ПЛИТ ОПЕРТЫХ НА ПОДАТЛИВЫХ РЕБРАХ

В работе представлен полуобратный метод получения полных решений тонких неоднородных пластических плит опертых на ребрах, которые прогибаются совместно с краями плиты. Плиты и ребра переходят в пластическое состояние согласно условию Губера—Мизеса и подлежат ассоциированному закону течения. Устройство нагружено поперечно равномерной нагрузкой и опирается в ребках. Получены полные решения для изотропных плит в форме квадрара, прямоугольника, ромба и параллелограмма. Рассмотрены тоже квадратные и прямоугольные ортотропные плиты. Полученние решения дают возможность проектировать неоднородные плиты, причем проектированная неоднородность гарантирует переход в полльное пластическое состояние целой конструкции в момент исчерпания насущей способности.

Разработано описание теории тонких пластических плит, подлежащих условию Губера—Мизеса, в неортогональной криволинейной системе координат. Затем специфицировано это описание для косоугольной системы прямолинейных координат, создавая пригодный инструмент для решения параллелограммных плит.

TECHNICAL UNIVERSITY OF WARSAW.

Received March 23, 1983.